Highlights

- Lower and upper flammability limits (LFL and UFL) and explosion pressures of binary alkane–N_2O mixtures are investigated.
- Binary alkane–N_2O mixtures exhibit smaller LFLs than corresponding binary alkane–O_2 mixtures.
- For binary alkane–N_2O mixtures, LFL and UFL can be predicted using the Le Chatelier's formulae.

1   **Flammability limits, explosion pressures, and applicability of Le Chatelier's rule to binary al-**

2   **kane–nitrous oxide mixtures**

3

4   Yusuke Koshiba [a, *], Takashi Hasegawa [b], Bongchan Kim [b], Hideo Ohtani [c]

5

6   [a] Department of Materials Science and Chemical Engineering, Faculty of Engineering, Yokohama

7   National University, 79-5 Tokiwadai, Hodogaya-ku, Yokohama 240-8501, Japan

8   [b] Department of Risk Management, Graduate school of Environmental and Information Sciences,

9   Yokohama National University, 79-7 Tokiwadai, Hodogaya-ku, Yokohama 240-8501, Japan

10   [c] Department of Safety Management, Faculty of Environmental and Information Sciences, Yoko-

11   hama National University, 79-7 Tokiwadai, Hodogaya-ku, Yokohama 240-8501, Japan

12

13   * Corresponding author   Telephone number: +81 45 339 3985

14   Fax number: +81 45 339 3985

15   E-mail address: ykoshiba@ynu.ac.jp, koshiba-yusuke-xm@ynu.ac.jp

16   Complete postal address: 79-5 Tokiwadai, Hodogaya-ku, Yokohama

17   240-8501, Japan

18

1 **Abstract**

2 This study investigates the flammability limits and explosion pressures of al-

3 kane–alkane–nitrous-oxide (N_2O) mixtures and corresponding alkane–alkane–O_2 mixtures at an ini-

4 tial pressure of 101.3 kPa and an initial temperature of approximately 20 °C. In addition, the present

5 study assesses whether Le Chatelier's rule holds for binary alkane mixtures in N_2O. In this study,

6 methane (CH_4), ethane (C_2H_6), propane (C_3H_8), n-butane (C_4H_{10}), and n-pentane (C_5H_{12}) were used

7 as fuels. The results clearly indicated that the lower and upper flammability limits of binary al-

8 kane–N_2O mixtures are smaller than those of the corresponding binary alkane–O_2 mixtures. Fur-

9 thermore, Le Chatelier's formula successfully predicted the lower and upper flammability limits of

10 binary alkane mixtures in N_2O.

11

12 Keywords: Nitrous oxide, Flammability limit, Explosion pressure, Le Chatelier's rule, Gas explosion,

13 Alkane

14

15

16

17

18

1

2 **Abbreviations**

3    $a_1–a_7$ Coefficients in the thermodynamic formulae

4   AFT Adiabatic flame temperature (K)

5   C Constant

6   c_p Heat capacity at constant pressure (J mol^{-1} K^{-1})

7    $c_{p, k}$ Heat capacity of product k at an adiabatic flame temperature (J mol^{-1} K^{-1})

8    $c_{p, total}$ Heat capacity for the total product at an adiabatic flame temperature (J mol^{-1}

9   K^{-1})

10   H Enthalpy (J mol^{-1})

11   ΔH_i Combustion enthalpy of fuel, i (kJ mol^{-1})

12   ΔH_{N2O} Decomposition enthalpy of nitrous oxide (kJ mol^{-1})

13   K_G Deflagration index (bar m s^{-1})

14   LFL Lower flammability limit (vol%)

15   LFL_T Lower flammability limit at a given temperature (vol%)

16   LFL_{T0} Lower flammability limit at ambient temperature (vol%)

17   n Number of fuels

18   P Explosion pressure (MPa)

| 1	*p*	Pressure (Pa)
2	*R*	Gas constant (J mol^{-1} K^{-1})
3	*S*	Entropy (J mol^{-1} K^{-1})
4	*T*	Temperature (K)
5	T_0	Ambient temperature (K)
6	*UFL*	Upper flammability limit (vol%)
7	x_i	Mole fraction of flammable gas, *i*, on a fuel basis (dimensionless)
8	$[x_k]$	Molar concentration of chemical species, *k* (mol m^{-3})
9	y_k	Mole fraction of product, *k* (dimensionless)
10		
11	*Greek letters*	
12	ϕ	Diameter (mm)
13		
14	*Subscripts*	
15	f	Fuel
16	mix	Mixture
17		
18		

1

2

3   **1. Introduction**

4

5   Chemical plants handling large amounts of flammable gases and liquids pose various risks (Pruph,

6   2016). Accidental explosions, fires, and chemical releases by the chemical industry may lead to cas-

7   ualties, environmental damage, and huge economic loss (Li et al., 2015; Gant and Atkinson, 2011;

8   CSB, 2007; Balasubramanian and Louvar, 2004; Wakakura and Iiduka, 1999); thus, such accidents

9   must be prevented. In particular, severe explosion accidents at chemical plants tend to attract con-

10 siderable public attention as they are highly publicized; this effect is known as the "social amplifica-

11 tion of risk" (Slovic, 2011). The social amplification framework indicates that the public's adverse

12 reactions and severe social impacts sometimes occur even if the risk events result in only minor

13 consequences. Hence, gaining an insight into the explosive characteristics (e.g., flammability limits

14 and explosion pressure) is of great help in ensuring safe operation.

15   A number of studies have reported the explosive characteristics of fuel–air and fuel–O_2 mixtures,

16 including their lower and upper flammability limits (*LFL* and *UFL*, respectively) and their explosion

17 pressures (*P*) (Britton, 2002; Pekalski et al., 2005). If the ignition energy is sufficient to initiate

18 flame propagation, the explosive characteristics generally depend on experimental conditions such as

5

1   initial temperature, initial pressure (Van den Schoor and Verplaetsen, 2006), vessel size and shape

2   (Razus et al., 2009), and quiescent or turbulent conditions. Cashdollar et al. (2000) reported that the

3   UFL value of a propane–air mixture in a 120 L chamber is slightly lower than that in a flammability

4   tube. Mashuga and Crowl (2000) revealed that deflagration index (K_G) values strongly depend on

5   humidity.

6   Nitrous oxide (N_2O, also known as laughing gas) is a colorless gas under ambient conditions and

7   has widely been used by industries as a nitriding and oxidizing gas (Imamura and Tokiwa, 2007;

8   Bose et al., 2000). Unfortunately, some accidental explosions caused by nitrous oxide have been re-

9   ported; for instance, a tank car explosion in the Netherlands injured 11 people and damaged the im-

10 mediate surroundings (Sonnemans and Körvers, 2006), and a gas cylinder explosion in Japan killed

11 two students and injured five people (Hirano, 2004). Such accidental explosions arise due to the na-

12 ture of nitrous oxide, i.e., it is thermodynamically unstable and its decomposition to N_2 and O_2 read-

13 ily commences at approximately 600 °C (Trogler, 1999) according to Eq. (1):

14

15                    $$N_2O \rightarrow N_2 + \frac{1}{2}O_2, \ \Delta H_{N_2O} = -82.1 \ \text{kJ/mol} ,$$ (1)

16
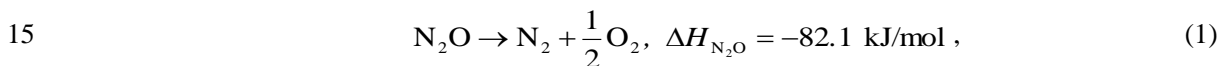
17 where ΔH_{N2O} is the decomposition enthalpy of N_2O.

18   To assess the risks of explosion, the estimation as well as point-by-point measurement of the

1 flammability limits and explosion pressures of these mixtures is crucial. For fuel–air mixtures, Eq.

2 (2) shows the relationship between the *LFL* and the enthalpy of combustion, ΔH_i, for a fuel, *i*, based

3 on the Burgess–Wheeler law (Rowley et al., 2010):

4

5
$$\Delta H_i = \frac{C}{LFL_i}. \tag{2}$$

6

7 where LFL_i is the LFL for fuel *i* and *C* is a constant. Here the total enthalpy of combustion of a mul-

8 tiple-fuel mixture, ΔH_{mix}, is given by

9

10
$$\Delta H_{\mathrm{mix}} = \sum x_i \Delta H_i, \tag{3}$$

11

12 where x_i is the mole fraction of flammable gas *i* on a fuel basis. Here, x_i obeys the following equa-

13 tion:

14

15
$$\sum_{i=1}^{n} x_i = 1. \tag{4}$$

16

17 Substituting Eq. (2) into Eq. (3) yields Le Chatelier's formula, a method for estimating LFLs (Coro-

18 nado et al., 2014):

7

1

$$LFL_{mix} = \frac{1}{\sum_{i=1}^{n} \frac{x_i}{LFL_i}}, \qquad (5)$$

2

3

4   where LFL_{mix} is the LFL for a flammable mixture. Even for elevated temperatures, Le Chatelier's

5   equation can be applied (Hustad and Sønju, 1988); furthermore, for the UFLs of mixtures in air, a

6   similar equation holds to some extent (Eq. (6)):

7

$$UFL_{mix} = \frac{1}{\sum_{i=1}^{n} \frac{x_i}{UFL_i}}, \qquad (6)$$

8

9

10 where UFL_i is the UFL for flammable gas i. Note that Le Chatelier's rule does not always hold for

11 upper-limit mixtures for mixtures containing unsaturated hydrocarbons (e.g., ethylene), diethyl ether,

12 and carbon monoxide (Zhao et al., 2009, Kondo et al., 2007). Thus, modifying the formula is often

13 required. Le Chatelier's formulae are used under the following inherent assumptions (Crowl and

14 Louvar, 2011a): the product heat capacities are constant, the combustion kinetics of the component

15 gases are independent of one another and unchanged, and the adiabatic flame temperature (AFT) of

16 each gas at its flammability limit is nearly identical.

17   Unlike fuel–air mixtures, few studies have been published on fuel–N_2O mixtures in the literature.

1   For instance, Pfahl et al. (2000) reported the flammability limits of H_2–N_2O–N_2, CH_4–N_2O–N_2,

2   NH_3–N_2O–N_2, and NH_3–N_2O–air mixtures at an initial pressure and temperature of 100 kPa and 295

3   K, respectively. Shebeko et al. (2003) demonstrated the flammability limits of CH_4–N_2O–CHF_3,

4   CH_4–O_2–N_2–CHF_3, and H_2–N_2O–fluorinated-hydrocarbon mixtures. Koshiba et al. (2010) reported

5   the flammability limits of $(C_2H_5)_2O$–N_2O, $(C_2H_5)_2NH$–N_2O, and C_3H_7CHO–N_2O mixtures. However,

6   it is unknown whether Le Chatelier's rule holds for fuel–N_2O mixtures.

7   The objectives of the present study are to experimentally investigate the flammability limits and

8   explosion pressures of fuel–fuel–N_2O (binary fuel–N_2O) mixtures at an initial pressure of 101.3 kPa

9   and an initial temperature of approximately 20 °C. This study employed five paraffinic hydrocarbons

10   (C_nH_{2n+2}) as fuels: methane (CH_4), ethane (C_2H_6), propane (C_3H_8), n-butane (n-C_4H_{10}), and

11   n-pentane (n-C_5H_{12}). In addition to their explosive characteristics, this study assessed whether Le

12   Chatelier's rule holds for binary alkane–N_2O mixtures.

13

14   **2. Material and Methods**

15

16   *2.1 Chemicals and gases*

17

18   The dry methane, ethane, propane, n-butane, nitrous oxide, oxygen, and nitrogen used in this study

9

1   have purities of >99.999, >99.7, >99.99, >99.95, >99.99, >99.99, and >99.99%, respectively.

2   n-Pentane (purity: >99.5%) was dried by passing through molecular sieves prior to use. All the fuels

3   and gases tested were used without further purification.

4

5   *2.2 Experimental procedures*

6

7   Fig. 1 illustrates the experimental apparatus, which is identical to that used for a previous study

8   (Koshiba et al., 2015). The closed, cylindrical stainless-steel vessel with a diameter of 100 mm and a

9   height of 120 mm includes a fan for stirring, two tungsten electrodes (ϕ 1.0 mm) for ignition, and

10   two pressure transducers. The pressure transducer (PGM-H, Kyowa Electronic Instruments Co., Ltd.,

11   Japan) placed on the side wall of the explosion vessel was used to observe the explosion pressure,

12   whereas another pressure transducer (PTI-S, Swagelok, USA) located on top of the vessel was used

13   to measure the partial pressures of the component gases.

14   Fig. 2 represents the flowchart of the explosion experiment. Prior to each explosion trial, the ex-

15   plosion vessel was sufficiently evacuated using a vacuum pump. The flammable mixtures were pre-

16   pared using the partial-pressure method and then well mixed using the fan at 1,000 rpm for one mi-

17   nute. Under the quiescent condition, each mixture was ignited at the center of the explosion vessel

18   with an electric-spark discharge between the electrodes; the igniter was consistently capable of

10

1   providing 18 J of energy. Each pressure history was recorded in a personal computer through a

2   measuring unit (NR-ST04 and NR-500, Keyence Co., Japan), and the spark discharge between the

3   electrodes was used as a trigger for recording data. In this study, a 7% pressure-rise criterion for ex-

4   plosion was employed, and all explosion trials were conducted at an initial pressure of 101.3 kPa and

5   an initial temperature of approximately 20 °C. Each measurement was repeated three times to con-

6   firm the reproducibility and the average explosion pressure for each mixture was determined fol-

7   lowing the three trials.

8

9   *2.3 Thermochemical equilibrium calculations*

10

11   In order to compute the adiabatic flame temperatures for lower- and upper-limit mixtures, thermo-

12   chemical equilibrium calculations were conducted using the CHEMKIN program (ver. 4.1.1, Kee et

13   al., 2007). For the mixtures not containing nitrogen, the following 26 chemical species were consid-

14   ered: C, CO, CO_2, CH, CH_2, CH_3, CH_4, C_2, C_2H_2, C_2H_4, C_2H_5, C_2H_6, C_3, C_4, C_5, C_6H_6, the fuel (i.e.,

15   CH_4, C_2H_6, C_3H_8, n-C_4H_{10}, and n-C_5H_{12}), H, H_2, OH, HO_2, H_2O, H_2O_2, O, O_2, and HCO. For the

16   mixtures containing N_2O or N_2, the following eight chemical species were further added: CN, N, N_2,

17   NO, NO_2, N_2O, NH, and HNO.

18   The thermodynamic coefficients (a_1–a_7) of the chemical species in the following equations were

11

1 extracted from the NASA Glenn Thermodynamic Database (2001).

2

$$\frac{c_p}{R} = \sum_{k=1}^{5} a_k T^{k-1} \; ; \tag{7}$$

4

$$\frac{H}{RT} = a_1 + \frac{a_2}{2}T + \frac{a_3}{3}T^2 + \frac{a_4}{4}T^3 + \frac{a_5}{5}T^4 + \frac{a_6}{T} \; ; \tag{8}$$

6

7

$$\frac{S}{R} = a_1 \ln T + a_2 T + \frac{a_3}{2}T^2 + \frac{a_4}{3}T^3 + \frac{a_5}{4}T^4 + \frac{a_7}{T} \; . \tag{9}$$

9

10 where c_p, R, a_1–a_7, T, H, and S are the heat capacity, gas constant, coefficients, temperature, enthalpy,

11 and entropy, respectively. The CHEMKIN program uses a general equation of state:

12

$$p = \sum_{k}[x_k]RT \; , \tag{10}$$

14

15 where p and $[x_k]$ are pressure and molar concentration of chemical species k, respectively.

16

17 **3. Results and discussion**

18

1	The explosion vessel used in this study is discussed here. In general, for explosion experiments, the

2	use of a standard vessel is recommended; for instance, ASTM (2015) employed a 5-L vessel and EN

3	1839 method B (2012) used a cylindrical or spherical vessel with a volume of >5 L. This is because

4	when a vessel is small, the influence of flame quenching at the vessel-wall surface (i.e., heat loss)

5	may not be negligible, perhaps narrowing the flammability range and reducing the observed explo-

6	sion pressure (Razus et al., 2006). The vessel volume in the present study is smaller than that of

7	standard vessels; in other words, the vessel used in this study has a higher surface-area to ves-

8	sel-volume ratio than that of the standard vessels described above. However, for a CH_4–air mixture,

9	the LFL and UFL values observed are nearly identical to the literature values (in the present study,

10	LFL: 5.2 vol%, UFL: 15.3 vol%; literature, LFL: ca. 5 vol%, UFL: ca. 15 vol%) (Kundu et al., 2016;

11	Crowl and Louvar, 2011b).

12

13	*3.1 Explosion pressure*

14

15	Fig. 3 shows the observed explosion pressures for the stoichiometric CH_4–C_5H_{12}–N_2O–N_2 mixtures.

16	In this section, the mixtures were diluted with 30-vol% N_2; in other words, the mixture was com-

17	posed of 70-vol% CH_4–C_5H_{12}–N_2O and 30-vol% N_2. The variable x_{CH4} represents the CH_4 mole

18	fraction in the fuel (i.e., CH_4–C_5H_{12}):

1

$$x_{CH_4} = \frac{CH_4}{CH_4 + C_5H_{12}}. \tag{11}$$

3

4 When x_{CH4} = 0, 0.25, 0.50, 0.75, and 1, the observed explosion pressures for the

5 CH$_4$–C$_5$H$_{12}$–N$_2$O–N$_2$ mixtures were found to be 1.52, 1.48, 1.45, 1.40, and 1.25 MPa, respectively.

6 Thus, the explosion pressure decreased gradually with an increase in x_{CH4}, which occurred because

7 n-pentane exhibits a higher reactivity than methane (Cashdollar et al., 2000). The adiabatic pressures

8 (i.e., the theoretical pressures determined by the thermochemical equilibrium calculations) and the

9 AFTs for the stoichiometric CH$_4$–C$_5$H$_{12}$–N$_2$O–N$_2$ mixtures are also plotted in this figure. The AFT

10 values were independent of x_{CH4}.

11　　Interestingly, there were no significant differences between the experimental and computed ex-

12 plosion pressures (maximum difference: ±0.04 MPa). The adiabatic pressure is generally higher than

13 the experimental explosion pressure because of heat losses (Salzano et al., 2012). Cashdollar et al.

14 (2000) reported that the experimental explosion pressures for methane–air mixtures are lower than

15 their calculated pressures despite using 20 L and 120 L explosion vessels. Zhang and Ng (2015)

16 clearly demonstrated that the experimental explosion pressures significantly differ from the corre-

17 sponding theoretical pressures for methane–dimethyl ether–air mixtures in a closed 20 L vessel.

18 However, as shown in this figure, the explosion pressures observed in this study agree well with the

14

1   adiabatic pressures computed using the CHEMKIN program. Thus, the result obtained from this

2   study is of great interest and reflects that the heat loss is negligible even when a relatively small ex-

3   plosion vessel is used.

4

5

6   *3.2 Lower flammability limit and the applicability of Le Chatelier's law*

7

8   Fig. 4 shows the variations of the LFLs as functions of x_{C2H6} for the C_2H_6–C_4H_{10}–N_2O mixtures. In

9   this study, the LFL is given on a vol% basis. The variable x_{C2H6} denotes the C_2H_6 mole fraction in

10   the fuel (i.e., C_2H_6–C_4H_{10}), varying from $x_{C2H6} = 0$ (i.e., pure C_4H_{10} in N_2O) to $x_{C2H6} = 1$ (i.e., pure

11   C_2H_6 in N_2O):

12

13                    $$x_{C_2H_6} = \frac{C_2H_6}{C_2H_6 + C_4H_{10}} \, .$$ (12)

14

15   The LFLs for the corresponding C_2H_6–C_4H_{10}–O_2 mixtures are also plotted. In this figure, open

16   squares and circles represent the LFLs for the mixtures containing N_2O and O_2, respectively. The

17   LFL values for the C_2H_6–C_4H_{10}–N_2O mixtures were determined to be 1.1, 1.2, 1.4, 1.4, 1.5, and 1.7

18   vol% when $x_{C2H6} = 0$, 0.2, 0.4, 0.6, 0.8, and 1.0, respectively. On the other hand, those for the

15

1   C_2H_6–C_4H_{10}–O_2 mixtures were 2.3, 2.5, 2.8, 3.0, 3.4, and 4.0 in the cases where x_{C2H6} = 0, 0.2, 0.4,

2   0.6, 0.8, and 1.0, respectively. The binary alkane–N_2O mixtures exhibited smaller LFLs than the

3   corresponding binary alkane–O_2 mixtures. Comparisons of the experimentally observed data (open

4   symbols) with the solid and dashed curves obtained from Eq. (5) clearly indicate that the experi-

5   mental data were successfully fitted by the calculated curves with an accuracy of ±0.1 vol%. We also

6   confirmed that Eq. (5) fits the observed LFL values for the CH_4–C_2H_6–N_2O, CH_4–C_3H_8–N_2O, and

7   CH_4–C_4H_{10}–N_2O mixtures, as well as for the corresponding CH_4–C_2H_6–O_2, CH_4–C_3H_8–O_2, and

8   CH_4–C_4H_{10}–O_2 mixtures (data not shown). Furthermore, Fig. 4 also shows that the adiabatic flame

9   temperatures for the lower-limit C_2H_6–C_4H_{10}–N_2O and C_2H_6–C_4H_{10}–O_2 mixtures were independent

10   of x_{C2H6}, which is due to the virtually identical AFTs for C_2H_6 and C_4H_{10} in N_2O at their LFLs.

11   Fig. 5 depicts the chemical compositions of the major chemical species with mole fractions of

12   >10^{-6} at the lower-limit C_2H_6–C_4H_{10}–N_2O mixture and total-product heat capacities calculated ac-

13   cording to Eq. (13).

14

15 $$c_{p,\,total} = \sum c_{p,k} \cdot y_k \,, \qquad\qquad (13)$$

16

17   where $c_{p,\,total}$, $c_{p,\,k}$, and y_k, are total-product heat capacity, heat capacity of product k, and mole frac-

18   tion of product species k. The calculations confirmed that the N_2O mole fraction was on the order of

16

1   10^{-6}, thus implying that almost all N_2O decomposed into O_2 and N_2 (according to Eq. (1)). As de-

2   scribed previously, Le Chatelier's formulae are derived using the assumption that the product heat

3   capacities are constant and the adiabatic flame temperature of each mixture at its flammability limit

4   is the same. As shown in this figure, each chemical composition remained constant for various val-

5   ues of x_{C2H6} and there were no significant differences in the heat capacities for the lower-limit mix-

6   tures containing N_2O. In addition, as stated previously, the adiabatic flame temperatures for the mix-

7   tures were nearly constant (see Fig. 4). Hence, Le Chatelier's rule was determined to hold for the

8   lower-limit C_2H_6–C_4H_{10}–N_2O mixtures. Needless to say, it does not hold in situations where low-

9   er-limit mixtures do not satisfy the assumptions.

10   A similar trend for the adiabatic flame temperatures and chemical compositions was observed for

11   the lower-limit C_2H_6–C_4H_{10}–O_2 mixtures.

12

13   *3.3 Upper flammability limit and the applicability of Le Chatelier's law*

14

15   Fig. 6 shows the UFLs as functions of x_{C2H6} for the C_2H_6–C_4H_{10}–N_2O and corresponding

16   C_2H_6–C_4H_{10}–O_2 mixtures. In this study, the UFL is given in terms of vol%. The variable x_{C2H6} also

17   represents the C_2H_6 mole fraction in the fuel (i.e., C_2H_6–C_4H_{10}), varying from 0 (i.e., pure C_4H_{10} in

18   N_2O) to 1 (i.e., pure C_2H_6 in N_2O). The UFL values for the C_2H_6–C_4H_{10}–N_2O mixture were found to

17

1   be 20.0, 31.5, 23.2, 25.4, 28.1, and 31.4 vol% when x_{C2H6} = 0, 0.2, 0.4, 0.6, 0.8, and 1.0, respectively.

2   However, the UFL values for the C_2H_6–C_4H_{10}–O_2 mixtures were 36.9, 38.6, 40.9, 43.4, 46.7, and

3   50.0 vol% in the cases where x_{C2H6} = 0, 0.2, 0.4, 0.6, 0.8, and 1.0, respectively. The binary al-

4   kane–N_2O mixtures exhibited smaller UFLs than the corresponding binary alkane–O_2 mixtures. As

5   shown in this figure, each curve calculated from Eq. (6) was adequate to predict the UFLs for the

6   C_2H_6–C_4H_{10}–N_2O and C_2H_6–C_4H_{10}–O_2 mixtures with an accuracy of ±0.4 vol%. We also confirmed

7   that Eq. (6) fits the observed LFL values for CH_4–C_3H_8–N_2O and the corresponding CH_4–C_3H_8–O_2

8   mixtures (data not shown). Adiabatic flame temperature calculations revealed nearly constant flame

9   temperatures for the C_2H_6–C_4H_{10}–N_2O and C_2H_6–C_4H_{10}–O_2 mixtures (C_4H_{10}–N_2O: 1833 K,

10   C_2H_6–N_2O: 1857 K and C_4H_{10}–O_2: 1413 K, C_2H_6–O_2: 1343 K).

11   Fig. 7 depicts the chemical composition of the main species with mole fractions of $>10^{-6}$ at the

12   upper-limit C_2H_6–C_4H_{10}–N_2O mixture. Although the mole fractions of H_2O (ca. 10^{-3}–10^{-2}) and CO_2

13   (ca. 10^{-4}–10^{-3}) increased with an increase in x_{C2H6}, no significant overall differences seemed to be

14   present among the x_{C2H6} = 0–1 mixtures. As seen in Figs. 6 and 7, the similar trends were observed

15   in the calculated equilibrium compositions and adiabatic flame temperatures for the upper-limit

16   C_2H_6–C_4H_{10}–N_2O mixtures to the lower-limit mixtures. The results regarding the AFTs, chemical

17   compositions, and total-product heat capacities clearly indicated that Le Chatelier's rule holds even

18   for the upper-limit C_2H_6–C_4H_{10}–N_2O mixtures.

1   Unfortunately, few data on the explosion properties of various fuel–nitrous-oxide mixtures are

2   available in the literature. Here, a comparison of limits of CH_4–N_2O mixtures is made. Table 1 sum-

3   marizes the LFL and UFL values of CH_4–N_2O mixtures given in the present study and the previous

4   study (Koshiba et al., 2015), together with their flammability limits reported in the literature

5   (Shebeko et al., 2013, Pfahl et al., 2000). Pfahl et al. and Shebeko et al. reported 2.5–3.0 vol% and

6   2.0 vol% of LFL for a CH_4–N_2O mixture, respectively. Thus, nearly the same LFL values, within

7   experimental error, were achieved in the literature and present study. For the UFL of the CH_4–N_2O

8   mixture, a UFL value of 42.4 vol% given in the present study also agreed well with the literature

9   values (Shebeko et al., 2013: 47.0 vol%; Pfahl et al., 2000: 43–50 vol%).

10   Note that, as described previously, the explosion properties of flammable mixtures vary depend-

11   ing on experimental conditions. For instance, lower flammability limits exhibit initial temperature

12   dependence and Eq. (14), which is also known as the modified Burgess–Wheeler rule, holds.

13

14
$$\frac{LFL_T}{LFL_{T_0}} = 1 - \frac{100 \cdot c_p \cdot (T - T_0)}{LFL_{T_0} \cdot (-\Delta H_f)} . \tag{14}$$

15

16   where LFL_T, LFL_{T0}, T_0, and ΔH_f are the lower flammability limit at a given temperature, lower

17   flammability limit at ambient temperature, ambient temperature, and combustion enthalpy of a fuel,

18   respectively. Chemical industries deal with flammable mixtures under various process conditions;

19

1   hence, further work is required to elucidate the influence of process conditions on the explosion

2   properties for alkane–N_2O mixtures.

3   In the chemical and process industries, avoiding flammable mixtures, preventing explosions

4   from starting, and mitigating the damage caused by an explosion are growing more important for

5   reducing the risks of explosion and fire. The preventive measurements include inerting (Chen et al.,

6   2009), reducing pressure (Coronado et al., 2014), and controlling fuel concentrations (Le et al.,

7   2013). In any case, for the flammable mixtures containing nitrous oxide, appropriate measurements

8   should be taken to reduce the risks of explosion and fire.

9

10   **4. Conclusions**

11

12   The present study experimentally investigated the flammability limits and explosion pressures for

13   binary alkane mixtures in N_2O at an initial pressure of 101.3 kPa and an initial temperature of ap-

14   proximately 20 °C; in addition, for binary alkane mixtures in N_2O, the applicability of Le Chatelier's

15   rule was evaluated. Based on the results presented in this study, the main conclusions are summa-

16   rized as follows:

17   1. Binary alkane–N_2O mixtures exhibited smaller LFL and UFL values than the corresponding

18   binary alkane–O_2 mixtures.

1   2. Le Chatelier's rule was found to hold for lower- and upper-limit binary alkane–N_2O mixtures,

2   thus allowing the prediction of their LFLs and UFLs.

3   3. The explosion pressures for binary alkane–N_2O mixtures were higher than those for the corre-

4   sponding binary alkane–O_2 mixtures.

5

6 The experimental results given in this study provide a clue to understanding the explosion character-

7 istics of fuels in nitrous oxide.

8

9 **References**

10 ASTM E 681-09, 2015. Standard test method for concentration limits of flammability of chemicals

11 (vapors and gases). Vol. 14.02. West Conshohocken, PA.

12

13 Balasubramanian, S.G., Louvar, J.F., 2004. Study of major accidents and lessons learned. Process

14 Saf. Prog. 21, 237–244.

15

16 Bose, M., Basa, D.K., Bose, D.N., 2000. Study of nitrous oxide plasma oxidation of silicon nitride

17 thin films. Appl. Surf. Sci. 158, 275–280.

18

21

1   Britton, L.G., 2002. Two hundred years of flammability limits. Process Saf. Prog. 21, 1–11.

2

3   Cashdollar, K.L., Zlochower, I.A., Green, G.M., Thomas, R.A., Hertzberg, M., 2000. Flammability

4   of methane, propane, and hydrogen gases. J. Loss Prev. Process Ind.13, 327–340.

5

6   Chen, C.-C., Wang, T.-C., Liaw, H.-J., Chen, H.-C., 2014. Nitrogen dilution effect on the flammabil-

7   ity limits for hydrocarbons, J. Hazard. Mater. 166 (2009) 880–890.

8

9   Coronado, C.J.R., Carvalho Jr, J.A., Andrade, J.C., Mendiburu, A.Z., Cortez, E.V., Carvalho, F.S.,

10   Gonçalves, B., Quintero, J.C., Gutiérrez Velásquez, E.I., Silva, M.H., Santos, J.C., Nascimento,

11   M.A.R., 2014. Flammability limits of hydrated and anhydrous ethanol at reduced pressures in aero-

12   nautical applications. J. Hazard. Mater. 280, 174–184.

13

14   Crowl, D.A., Louvar, J.F., 2011a. Chemical Process Safety: fundamentals with applications, 3rd ed.

15   Pearson Education, Inc. Boston, pp. 253–254.

16

17   Crowl, D.A., Louvar, J.F., 2011b. Chemical Process Safety: fundamentals with applications, 3rd ed.

18   Pearson Education, Inc. Boston, p. 654.

1

2   EN 1839 method B, 2012. Determination of explosion limits of gases and vapours. Sec 4.1. Brussels.

3

4   Gant, S.E., Atkinson, G.T., 2011. Dispersion of the vapour cloud in the Buncefield incident. Process

5   Saf. Env. Prot. 89, 391–403.

6

7   Hirano, T., 2004. Accidental explosions of semiconductor manufacturing gases in Japan. J. Loss Prev.

8   Process Ind. 17, 29–34.

9

10   Hustad, J.E., Sønju, O.K., 1988. Experimental studies of lower flammability limits of gases and

11   mixtures of gases at elevated temperatures. Combust. Flame 71, 283–294.

12

13   Imamura, K., Tokiwa, H., 2007. Theoretical study of N_2O adsorption on clean and partially oxidized

14   Si(100)-(2×1) small clusters. Chem. Phys. Lett. 436, 263–267.

15

16   Kee, R.J., Rupley, F.M., Miller, J.A., Coltrin, M.E., Grcar, J.F., Meeks, E., Mof-fat, H.K., Lutz, A.E.,

17   Dixon-Lewis, G., Smooke, M.D., Warnatz, J., Evans, G.H., Larson, R.S., Mitchell, R.E., Petzold,

18   L.R., Reynolds W.C., Caracotsios, M., Stew-art, W.E., Glarborg, P., Wang, C., McLellan, C.L., Adi-

1 gun, O., Houf, W.G., Chou, C.P., Miller, S.F., Ho, P., Young, P.D., Young, D.J., Hodgson, D.W.,

2 Petrova, M.V., Puduppakkam, K.V., 2007. CHEMKIN Release 4.1.1, Reaction Design, San Diego,

3 CA.

4

5 Kondo, S., Takizawa, K., Takahashi, A., Tokuhashi, K., Sekiya, A., 2007. Flammability limits of

6 isobutane and its mixtures with various gases. J. Hazard. Mater. 148, 640–647.

7

8 Koshiba, Y., Nishida, T., Morita, N., Ohtani, H., 2015. Explosion behavior of n-alkane/nitrous oxide

9 mixtures. Process Saf. Env. Prot. 98, 11–15.

10

11 Koshiba, Y., Takigawa, T., Matsuoka, Y., Ohtani, H., 2010. Explosion characteristics of flammable

12 organic vapors in nitrous oxide atmosphere. J. Hazard. Mater. 183, 746–753.

13

14 Kundu, S., Zanganeh, J., Moghtaderi, B., 2016. A review on understanding explosions from me-

15 thane–air mixture. J. Loss Prev. Process Ind. 40, 507–523.

16

17 Le, H., Liu, Y., Mannan, M.S., 2013. Lower flammability limits of hydrogen and light hydrocarbons

18 at subatmospheric pressures, Ind. Eng. Chem. Res. 52, 1372–1378.

1

2   Li, X., Koseki, H., Mannan, M.S., 2015. Case study: Assessment on large scale LPG BLEVEs in the

3   2011 Tohoku earthquakes, J. Loss Prev. Process Ind. 35, 257–266.

4

5   Mashuga, C.V., Crowl, D.A., 2000. Problems with identifying a standard procedure for determining

6   KG values for flammable vapors. J. Loss Prev. Process Ind. 13, 369–376.

7

8   NASA Thermo Build, 2001. http://www.grc.nasa.gov/WWW/CEAWeb/ceaThermoBuild.htm (Ac-

9   cessed 04.07.16).

10

11   Pekalski, A.A., Schildberg, H.P., Smallegange, P.S.D., Lemkowitz, S.M., Zevenbergen, J.F.,

12   Braithwaite, M., Pasman, H.J., 2005. Determination of the explosion behaviour of methane and pro-

13   pene in air or oxygen at standard and elevated conditions. Process Saf. Env. Prot. 83, 421–429.

14

15   Pfahl, U.J., Ross, M.C., Shepherd, J.F., 2000. Flammability limits, ignition energy, and flame speeds

16   in H_2–CH_4–NH_3–N_2O–O_2–N_2 mixtures. Combust. Flame 123, 140–158.

17

18   Pruph, R.W., 2016. Life-safety concerns in chemical plants. Process Saf. Prog. 35, 18–25.

1

2   Razus, D., Brinzea, V., Mitu, M., Oancea, D., 2009. Explosion characteristics of LPG–air mixtures in

3   closed vessels. J. Hazard. Mater. 165, 1248–1252.

4

5   Razus, D., Movileanu, C., Brinzea, V., Oancea, D., 2006. Explosion pressures of hydrocarbon–air

6   mixtures in closed vessels. J. Hazard. Mater. B135, 58–65.

7

8   Rowley, J.R., Rowley, R.L., Wilding, W.V., 2010. Experimental determination and re-examination of

9   the effect of initial temperature on the lower flammability limit of pure liquids. J. Chem. Eng. Data

10   55, 3063–3067.

11

12   Salzano, E., Cammarota, F., Di Benedetto, A., Di Sarli, V., 2012. Explosion behavior of hydro-

13   gen-methane/air mixtures. J. Loss Prev. Process Ind. 25, 443–447.

14

15   Shebeko, A.Y., Shebeko, Y.N., Zuban, A.V., Navzenya, V.Y., 2013. An experimental investigation of

16   an inertization effectiveness of fluorinated hydrocarbons in relation to premixed H_2–N_2O and

17   CH_4–N_2O flames. J. Loss Prev. Process Ind. 26, 1639–1645.

18

1   Slovic, P., 2011. The perception of risk, in: Kasperson, R.E., Renn, O., Slovic, P., Brown, H.S., Emel,

2   J., Goble, R., Kasperson, J.X., Ratick, S. (Eds.), The social amplification of risk: a conceptual

3   framework. Earthscan Publications, London, 232–245.

4

5   Sonnemans, P.J.M., Körvers, P.M.W., 2006. Accidents in the chemical industry: are they foreseea-

6   ble? J. Loss Prev. Process Ind. 19, 1–12.

7

8   Trogler, W.C., 1999. Physical properties and mechanisms of formation of nitrous oxide. Coord.

9   Chem. Rev. 187, 303–327.

10

11 U.S. Chemical Safety and Hazard Investigation Board, 2007. Final investigation report: refinery ex-

12 plosion and fire.

13

14 Van den Schoor, F., Verplaetsen, F., 2006. The upper explosion limit of lower alkanes and alkenes in

15 air at elevated pressures and temperatures. J. Hazard. Mater. A128, 1–9.

16

17 Wakakura, M., Iiduka, Y., 1999. Trends in chemical hazards in Japan. J. Loss Prev. Process Ind. 12,

18 79–84.

1

2   Zhang, B., Ng, H.D., 2015. Explosion behavior of methane–dimethyl ether/air mixtures. Fuel 157,

3   56–63.

4

5   Zhao, F., Rogers, W.J., Mannan, M.S., 2009. Experimental measurement and numerical analysis of

6   binary hydrocarbon mixture flammability limits, Process Saf. Env. Prot. 87, 94–104.

7   **Figure captions**

8

9   Figure 1

10   Schematic of the experimental apparatus for the explosion tests.

11

12   Figure 2

13   Flowchart of the explosion experiment.

14

15   Figure 3

16   The observed explosion pressures ($\circ$), computed adiabatic pressures (solid curve), and adiabatic

17   flame temperatures (dashed curve) for the stoichiometric CH_4–C_5H_{12}–N_2O–N_2 mixtures. The varia-

18   ble x_{CH4} denotes the CH_4 mole fraction in the fuel CH_4–C_5H_{12}. As described in the text, the N_2 con-

1 centration was fixed at 30 vol%.

2

3 Figure 4

4 Values of LFL and AFT for the C_2H_6–C_4H_{10}–N_2O and C_2H_6–C_4H_{10}–O_2 mixtures as functions of the

5 C_2H_6 mole fractions in the fuels. The open and closed symbols denote the LFLs and AFTs, respec-

6 tively. The square and circle symbols represent the lower-limit C_2H_6–C_4H_{10}–N_2O and

7 C_2H_6–C_4H_{10}–O_2 mixtures, respectively. The dashed and solid curves are calculated from Eq. (5) for

8 the lower-limit C_2H_6–C_4H_{10}–N_2O and C_2H_6–C_4H_{10}–O_2 mixtures, respectively.

9

10 Figure 5

11 Calculated equilibrium compositions for lower-limit C_2H_6–C_4H_{10}–N_2O mixtures. In this figure, only

12 the main chemical species with mole fractions of $>10^{-6}$ were plotted against x_{C2H6} ($x_{C2H6} = 0$: pure

13 C_4H_{10} in N_2O and $x_{C2H6} = 1.0$: pure C_2H_6 in N_2O). The solid curve represents the total-product heat

14 capacity for lower-limit C_2H_6–C_4H_{10}–N_2O mixtures, which is calculated from Eq. (13).

15

16 Figure 6

17 UFL and AFT values for C_2H_6–C_4H_{10}–N_2O and C_2H_6–C_4H_{10}–O_2 mixtures as a function of the C_2H_6

18 mole fraction in the fuels. The open and closed symbols denote the UFLs and AFTs, respectively.

1 The lozenge and hexagonal symbols represent the upper-limit C_2H_6–C_4H_{10}–N_2O and

2 C_2H_6–C_4H_{10}–O_2 mixtures, respectively. The dashed and solid curves are calculated from Eq. (6) for

3 the upper-limit C_2H_6–C_4H_{10}–N_2O and C_2H_6–C_4H_{10}–O_2 mixtures, respectively.

4

5 Figure 7

6 Calculated equilibrium compositions for upper-limit C_2H_6–C_4H_{10}–N_2O mixtures. In this figure, only

7 the main chemical species with mole fractions of $>10^{-6}$ are plotted against x_{C2H6} (x_{C2H6} = 0: pure

8 C_4H_{10} in N_2O and x_{C2H6} = 1.0: pure C_2H_6 in N_2O). The solid curve represents the total-product heat

9 capacity for upper-limit C_2H_6–C_4H_{10}–N_2O mixtures, which is calculated from Eq. (13).

10

11

12

13

14

15

16

17

18

1

2

3

4

5

6   **Table caption**

7   Table 1

8   Lower and upper flammability limits for the methane–nitrous-oxide mixture.

Table 1

		Shebeko et al., 2013	Pfahl et al., 2000	Koshiba et al., 2015
LFL (vol%)		2.0	2.5–3.0	2.5
UFL (vol%)		47.0	43–50	42.4
Experimental condition	Initial temperature	Ambient temperature	295 K	293 K
	Initial pressure	1 atm	100 kPa	101.3 kPa
	Ignition energy (J)	2	8	18
	Vessel volume (L)	4.2	11.25	0.94

Figure 1
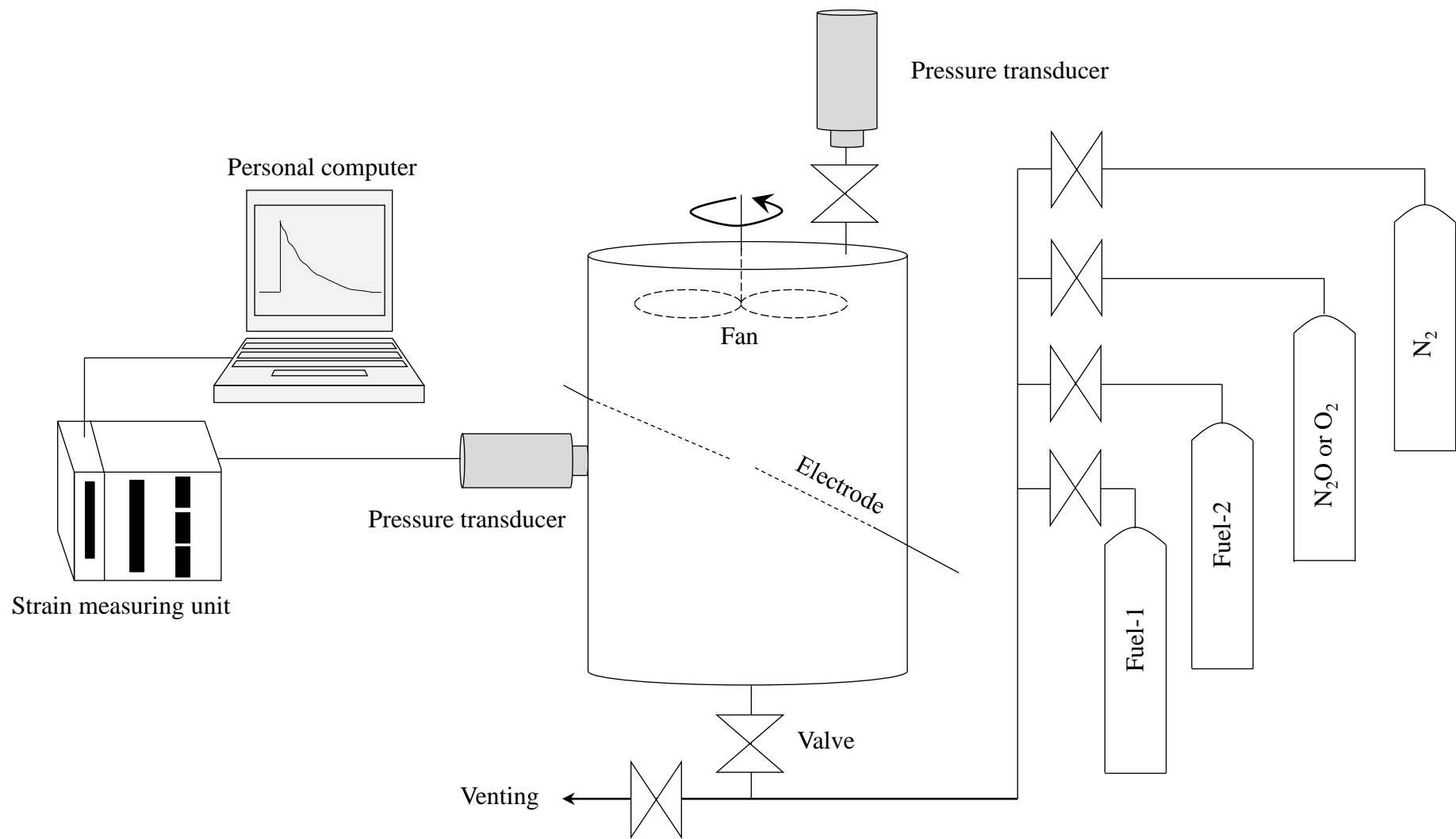
Figure 2
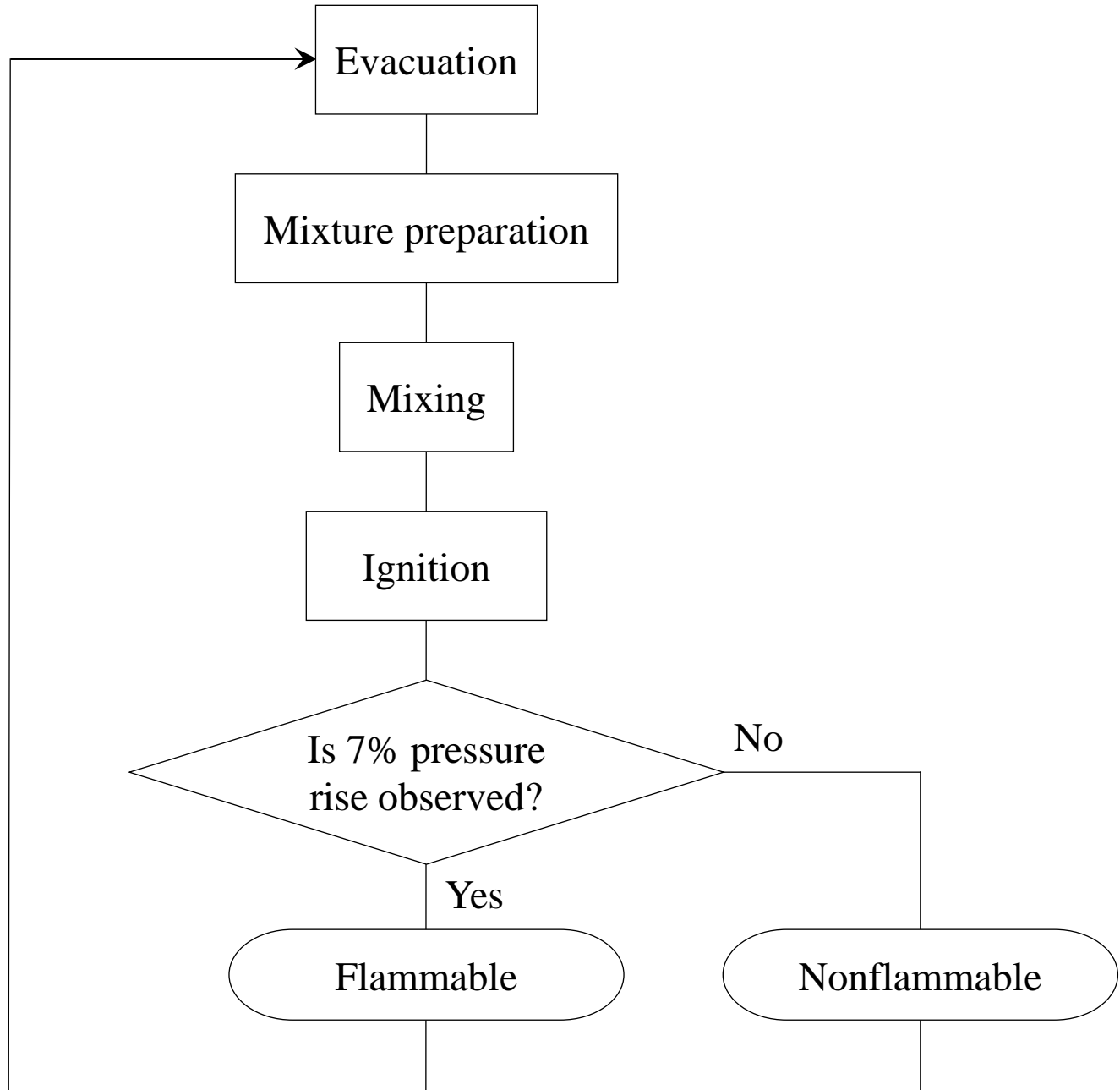
Figure 3
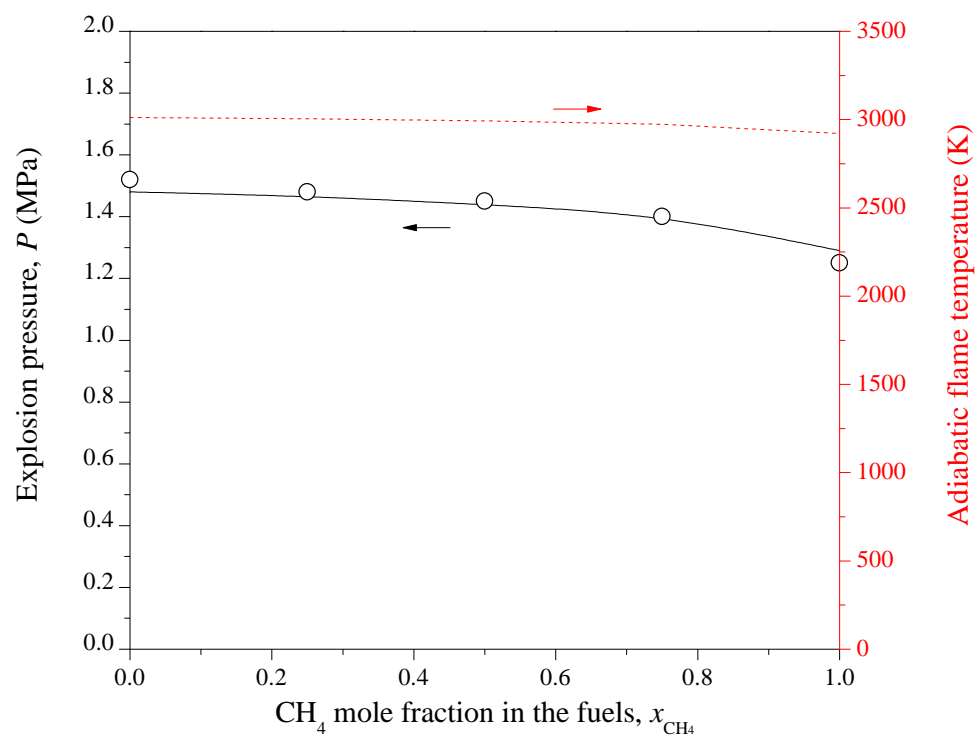
Figure 4
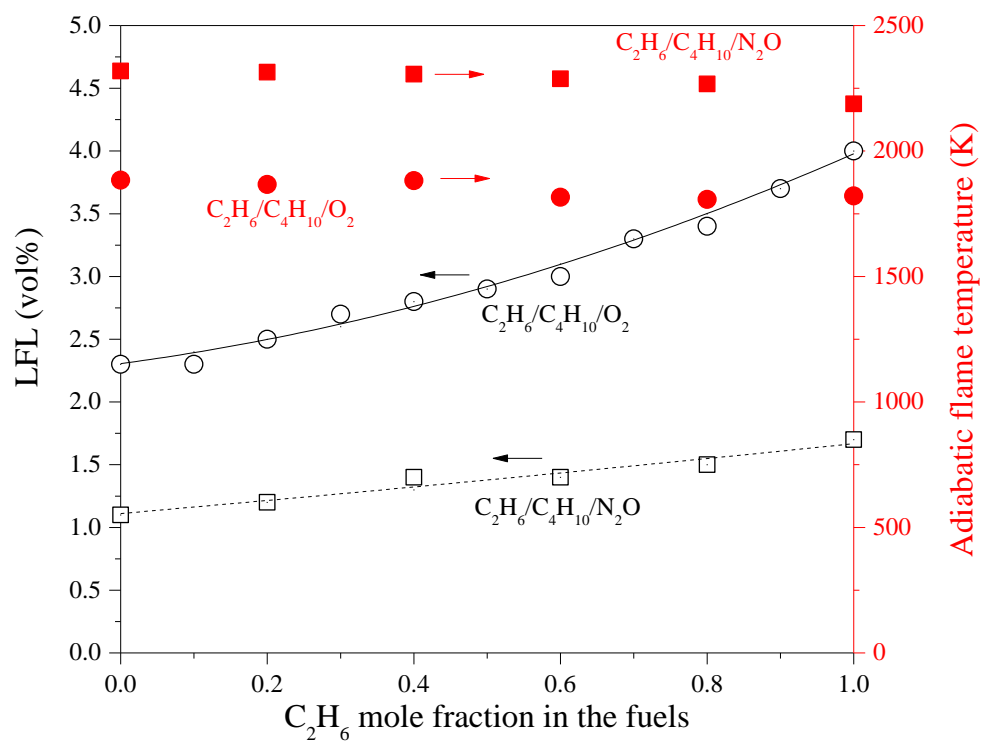
Figure 5

Figure 6

Figure 7